Journal Pre-proofs

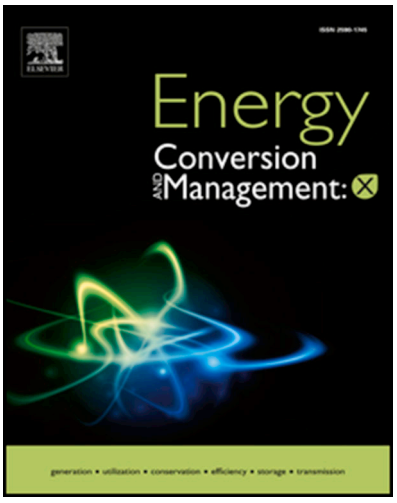

Bio-jet fuel production from crude palm kernel oil under hydrogen-nitrogen atmosphere in a fixed-bed reactor by using Pt/C as catalyst

Worada Moonsrikaew, Nattee Akkarawatkhoosith, Tiprawee Tongtummachat, Amaraporn Kaewchada, Kun-Yi Andrew Lin, Rabrov Evgeny, Attasak Jaree

PII: S2590-1745(23)00127-7
DOI: https://doi.org/10.1016/j.ecmx.2023.100471
Reference: ECMX 100471

To appear in: *Energy Conversion and Management: X*

Received Date: 26 June 2023
Revised Date: 28 September 2023
Accepted Date: 5 October 2023

Please cite this article as: W. Moonsrikaew, N. Akkarawatkhoosith, T. Tongtummachat, A. Kaewchada, K-Y. Andrew Lin, R. Evgeny, A. Jaree, Bio-jet fuel production from crude palm kernel oil under hydrogen-nitrogen atmosphere in a fixed-bed reactor by using Pt/C as catalyst, *Energy Conversion and Management: X* (2023), doi: https://doi.org/10.1016/j.ecmx.2023.100471

Bio-jet fuel production from crude palm kernel oil under hydrogen-nitrogen atmosphere in a fixed-bed reactor by using Pt/C as catalyst

Worada Moonsrikaew[1], Nattee Akkarawatkhoosith[2], Tiprawee Tongtummachat[2], Amaraporn Kaewchada[3], Kun-Yi Andrew Lin[4], Rabrov Evgeny[5], Attasak Jaree[1,*]

[1] Center of Excellence on Petrochemical and Materials Technology, Department of Chemical Engineering, Faculty of Engineering, Kasetsart University, Chatuchak, Bangkok, Thailand

[2] Department of Chemical Engineering, Faculty of Engineering, Mahidol University Nakhon Pathom, Thailand

[3] Department of Agro-industrial, Food, and Environmental Technology, King Mongkut's University of Technology North Bangkok, Bandsue, Bangkok, Thailand

[4] Department of Environmental Engineering & Innovation and Development Center of Sustainable Agriculture, National Chung Hsing University, Taichung, Taiwan

[5] School of Engineering, University of Warwick, Coventry, United Kingdom

***Corresponding Author:** Attasak Jaree, Department of Chemical Engineering, Faculty of Engineering, Kasetsart University, Chatuchak, Bangkok, 10900, Thailand.

E-mail: fengasj@ku.ac.th

Abstract

This research presents a study on the production of biojet fuel using crude palm kernel oil (CPKO) as a novel source. The aim of the research is to explore an efficient and high-throughput process for biojet production from CPKO. The experiment was conducted using a reactor packed with 5 wt.% platinum on carbon (Pt/C). Several key operating variables, such as reaction temperature, hydrogen-to-nitrogen ratio, pressure, gas flow rate, and CPKO flow rate, were investigated to optimize the yield of liquid product and biojet fuel. The

optimal conditions determined were a reaction temperature of 400ºC, pressure of 500 psi, CPKO flow rate of 0.02 mL/min, hydrogen-to-nitrogen ratio of 75:25, and gas flow rate of 25 mL/min. Under these conditions, the biojet fuel yield reached 59%, with a productivity of 330.6 $g_{product}/g_{cat}$-h. The results demonstrated superior production performance compared to other existing processes in the field.

Keyword: Aviation biofuel, continuous process, process intensification, heterogenous catalyst, hydroprocessing

1. Introduction

Countries worldwide are facing environmental challenges associated with energy resources and their conversion. Presently, fossil fuels remain the primary sources of energy, leading to substantial greenhouse gas (GHG) emissions and global climate change. In 2018, global energy consumption reached approximately 270.5 exajoules, resulting in over 33 billion tonnes of CO_2 emissions [1]. Jet fuel plays a vital role as a transportation fuel, driven by advancements in the aviation industry. Unfortunately, the predominant production of jet fuel from petroleum sources contributes to the accumulation of greenhouse gases in the Earth's atmosphere. Shifting from petroleum-based fuel to bio-based alternatives is highly desirable for sustainable biojet fuel. However, the current state of biojet production faces challenges in terms of technical and economic competitiveness, necessitating further exploration and development [2].

Lignocellulosic biomass offers potential for biojet production through various technologies, including hydrolysis and Fischer-Tropsch processes [3]. These conversion methods have been widely adopted for large-scale production, particularly the oil-to-jet conversion pathway. Among these approaches, the hydroprocessing process is recognized as the optimal solution for sustainable biojet production [4]. Consequently, this research focuses

on the conversion of low-value triglycerides into biojet fuel through hydroprocessing, involving a series of reactions such as dehydration, hydrodeoxygenation (HDO), and decarboxylation (DCX) [5].

Biojet fuel typically consists of hydrocarbons within the carbon range of C_6-C_{18}, with an aromatic content of less than 25%. However, biojet fuel obtained through a single process often requires further upgrading, such as isomerization and aromatization, to meet the specifications of commercial aviation fuel (Jet A-1). Ensuring the freezing point below -47°C is particularly crucial to provide optimal flow properties at high altitudes [6]. Among various sources of triglycerides, including soybean oil, palm oil, rice bran oil, etc., each with distinct fatty acid profiles, crude palm kernel oil (CPKO) has been regarded as a promising and abundant carbon source for biojet production due to the significant amounts of dodecanoic acid (C12:0), tetradecanoic acid (C14:0), hexadecenoic acid (C16:0), and oleic acid (C18:1). CPKO offers advantages such as availability, cost-effectiveness, and abundance compared to medium-chain oils like coconut oil. As a result, CPKO was selected as the raw material for this study.

The catalyst used in the production of biojet fuel plays a critical role in achieving the high biojet yield. Various types of solid catalysts have been explored in the literature. For example, tantalum phosphate (TaPa) was synthesized and reported by Rambabu et al., (2023) [7] as one of the effective catalysts for hydrotreating process. In their work, the date palm seed bio-oil was catalytically converted at 400ºC and 10 bar of H_2 to produce 53.6% of bio-jet fuel (C_9-C_{15}) and 35.9% of green diesel (C_{14}-C_{20}). The Ni_3Fe bimetallic hybrid catalyst synthesized by Bharath et al. (2020) [8] was also reported as effective for the upgrading of biofuel via hydrodeoxygenation. However, further research of these catalysts is still necessary for the bulk catalyst production. Using commercial catalysts might be the shortest way to approach to the commercial biojet production. Commercial catalysts such as palladium or platinum on supported catalysts, i.e. Pt/Al_2O_3 and Pd/C, have been used for deoxygenation process of vegetable oil to bio jet fuel [9]. For example, the Pd/C catalyst was applied in the work of Why et al. (2021) [10] for biojet production from palm kernel oil. About 96% of liquid yield was achieved with the 73% of biojet selectivity. However, the large amount of catalyst (8 wt.% of catalyst mass) was required the achieve the high biojet yield. Similar result was found in the work of Zhang and Chen (2015) [11], who used Pd supported catalysts (20 wt.% of catalyst mass) for biojet production from plam oil. Using these commercial catalysts also require further development for the economic feasibility of production.

The cost of raw materials represents a significant portion of the overall cost of biojet production [12, 13], posing challenges to the economic feasibility of commercial biojet fuel production. In the oil-to-jet production route, the cost-effective utilization of oil-based materials (carbon source) and hydrogen gas as the primary feedstocks is crucial. While pure hydrogen is required to achieve high biojet yields, its cost must be carefully balanced. One potential approach for cost optimization is the use of a gas mixture comprising low-cost gases, such as nitrogen, in combination with hydrogen. It is worth noting that the price of

hydrogen is approximately 2 $/kg, whereas nitrogen is priced at around 0.2 $/kg [14]. However, the impact of gas mixture on biojet yield needs to be thoroughly investigated.

In this study, a continuous fixed-bed reactor packed with Pt/C catalyst was utilized for the conversion of CPKO into biojet fuel. Both hydrogen and nitrogen atmospheres were employed to evaluate the feasibility of biojet production. To our knowledge, there has been no research conducted on the application of nitrogen gas or a nitrogen/hydrogen gas mixture for biojet production in a flow reactor. The influence of key reaction variables, including temperature, hydrogen-to-nitrogen ratio, pressure, gas flow rate, and CPKO flow rate, on the liquid product yield and biojet yield, was systematically investigated and optimized. The performance of the reactions under the optimal conditions was compared with existing literature.

2. Materials and methods

2.1 Materials

The crude palm kernel oil used in this study was provided by Univanich Palm Oil Public Company Ltd., located in Krabi, Thailand. Prior to experimentation, the oil sample underwent degassing using ultrasonic treatment and was stored in an amber glass bottle to prevent light-induced oxidation reactions. For the experimental setup, a steam coil heating tape was used to maintain the feedstock temperature at 60°C. The characterization of the feedstock was conducted using gas chromatography-mass spectrometry (GC-MS) analysis, employing a nonpolar phase DB-5HT column (30 m x 0.25 mm x 0.25 µm) with 5% diphenyl-95% dimethyl siloxane.

The catalyst used in this study was 5% platinum supported on activated carbon (Pt/C). It was obtained from Riogen, USA, with an assay of >98% purity. Glass wool with a low lead content was provided by Chem-supply. Isopropanol (AR grade, 99.7%) was purchased from QReC. Sodium sulfate anhydrous (99.0%) and potassium hydroxide pellets (85%) were obtained from Carlo-Erba. Ultra-high purity helium (99.999%), compressed air (air zero), and high-purity hydrogen (99.99%) were supplied by Linde (Thailand).

2.2 Catalysts characterization

The nitrogen adsorption-desorption isotherms at -196°C were analyzed to determine the catalyst textural properties. The Brunauer-Emmett-Teller theory (BET) was applied to calculate the surface area, pore volume, and pore diameter of the catalysts. Nitrogen physisorption measurements were performed using a Micrometrics unit (version 3Flex 5.02). The total pore volume and average pore size were determined using the Barrett-Joyner-Halenda (BJH) method.

To determine the reduction temperature of the catalysts, hydrogen temperature-programmed reduction (H_2-TPR) was carried out. The measurement was conducted using Microactive for AutoChem II (version 6.01). Approximately 0.2 g of the Pt/C catalyst was used for the measurement. A mixture of 10% H_2/Ar was introduced at a flow rate of 30 mL/min into the sample loop and served as the reference gas as well. The sample was heated at a rate of 5 °C/min up to 800°C. Gas analysis was performed using mass spectrometry.

The NH_3 temperature-programmed desorption (NH_3-TPD) analysis was performed using the Micromeritics 3 Flex analyzer (version 5.2). For each experiment, a catalyst sample size of 150-200 mg was subjected to a 1 h treatment at 900°C with a 10 mol% H_2/Ar gas mixture flowing at a rate of 30 cm^3/min. The sample was then cooled to 150°C and exposed to a gas mixture of 97 mol% NH_3 and 3 mol% He at a flow rate of 30 cm^3/min for 1 h to saturate the catalyst. Subsequently, the flow of NH_3 was stopped, and the catalyst was purged with pure inert gas (He) at a flow rate of 30 cm^3/min at 100°C for an additional hour to remove physically adsorbed NH_3. The temperature was then raised to 900°C while gradually desorbing NH_3 at a rate of 10°C/min. The concentration of NH_3 in the effluent gas was monitored using a thermal conductivity detector (TCD).

To investigate the catalyst structure, X-ray diffractometer analysis (XRD) was conducted using a PANalytical X'Pert PRO instrument located in Almelo, Netherlands. The catalyst sample was pulverized and placed on a stainless steel plate. The diffraction patterns were captured in stages using a Cu/K-alpha1 radiation source with settings of 40 kV and 30 mA, and a wavelength (λ) of 1.5406. The range of Bragg angle 2-theta (2θ) for data collection was between 20-80°. The crystal structure was determined using the ICDD PDF-2 database (2011 version).

To examine the surface morphology and metal dispersion on the support, scanning electron microscope (SEM) combined with energy-dispersive X-ray spectrometer (EDS) analysis was performed on the 5% platinum supported on activated carbon catalyst. The JSM-7600F microscope, offering excellent resolution with energy dispersive X-ray capabilities ranging from 0.1 to 30 kV and magnifications from 25 to 1,000,000x, was used to capture micrographs of the fresh catalysts.

2.3 Biojet production

Figure 1 illustrates the experimental setup used in this study. Prior to the reaction tests, the Pt/C catalyst underwent treatment at 330°C with a hydrogen flow rate of 70 mL/min for 90 min. The experiment was carried out based on our previous work [15]. The crude palm kernel oil was introduced into a fixed-bed reactor with dimensions of 4.6 mm ID x 5 mm length, utilizing a high-performance liquid chromatography (HPLC) pump to control the specific flow rate (see Table 1). This oil stream was then mixed with hydrogen gas in a J-mixer, and the combined mixture entered the fixed-bed reactor, facilitating the chemical reactions. The system pressure was regulated by a back-pressure regulator located at the exit

end of the reactor. Subsequently, the product underwent separation into gas, oil, and water phases. Periodic collection of liquid samples occurred over a duration of 10 h. To eliminate water from the oil product, sodium sulfate (Na_2SO_4) was employed, and the samples were stored at -20°C for subsequent analysis. For each experiment, Pt/C catalyst was used in the amount of 0.04 g. The reaction conditions for each experiment are presented in Table 1.

2.4 Liquid product characterization

The collected samples were subjected to sodium sulfate anhydrous treatment to remove water content prior to analysis. The composition of the oil samples was determined using a gas chromatograph equipped with a flame ionization detector (HP6890, Agilent) and a DB-5HT column. The oven temperature was programmed to increase from an initial temperature of 50°C, held for 2 min, then ramped up to 130°C at a rate of 10 °C/min, followed by a further increase to 365°C at a rate of 15 °C/min. The temperature was then maintained at 365°C for 15 min. Both the flame ionization detector and injector were set to 350°C. A 1 µL sample was injected into the column using a 40:1 split ratio. Helium was used as the carrier gas at a constant flow rate. The analysis results were used to determine the product yield (n-alkanes; nC_8-nC_{16}) and productivity ($g_{product}/g_{cat}$-h), as shown in Equations 1 and 2, respectively.

$$\%\text{Yield (n-C}_8\text{ to n-C}_{16}) = \frac{\%\text{area of n-C}_8\text{ to n-C}_{16}\text{ x weight of oil product}}{\text{weight of CPKO}} \quad (1)$$

$$\text{Productivity} = \frac{\%\text{area x weight of oil product}}{\text{amount of active catalyst x time}} \quad (2)$$

3. Results and discussion

3.1 Catalysts characterization

Various studies on the characterization of Pt/C catalyst were performed to support its performance in our biojet production system. The first set of properties investigated were the textural properties, which were assessed using the N_2 adsorption-desorption method based on the BET and BJH methods. The summarized results can be found in Table S1 (supplementary section), while the N_2 adsorption/desorption isotherm is shown in Figure S1.

The BET analysis revealed favorable mesoporous characteristics of the Pt/C catalyst, making it suitable for the deoxygenation reaction [16]. Compared to other catalysts used in deoxygenation reactions (see Table S1), the Pt/C catalyst exhibited a higher surface area (994.9 m^2/g). High surface area offered the high accessibility of the reactants to the surface of catalyst active site, promoting the rate of reaction [17].

Another important property studied was the reducibility of the Pt species on the carbon support, which was assessed using H_2-TPR [18]. The results are depicted in Figure S2(a). Three distinct hydrogen consumption zone profiles were observed for the Pt/C catalyst. The first principal reduction peak, appearing at 180°C, indicated the reduction of a Pt-supported metal complex that had been deposited on carbon with varying degrees of surface oxidation. At reduction temperatures of 320°C and 400°C, the Pt species demonstrated a transition from a divalent state to a zerovalent state. The high-temperature H_2-consumption zone coincided with the desorption peak of CO, as indicated by the significant decrease at 600°C. Temperatures above 600°C indicated that transition metals could act as catalysts for methane synthesis through the reaction of hydrogen with carbon, while the shoulder peak around 550°C was attributed to the gasification of the carbon support. It should be noted that due to the strong interaction between the metal and support at high temperatures, doped metal oxides could not be fully reduced. Therefore, in this work, the catalyst was reduced at 330°C, in line with the findings of Bangjang et al. (2020) [19].

The acidity of the catalyst was analyzed using NH_3-TPD, as depicted in Figure S2(b). The desorption profile of ammonia exhibited a broad peak ranging from 600°C to 900°C. The first peak, observed at 680°C, resulted from the partial oxidation of carbon and remained relatively constant within the range of 700-800°C. The second peak, appearing at 860°C, indicated the presence of a small amount of strong acidic sites of the catalyst. Additionally, the temperature of the desorption peak provided information about the relative strength of the acidic or basic sites [20].

The XRD pattern of cubic Pt/C given from ICDD PDF Card No. 01-089-7282 exhibited diffraction peaks at 2θ (40-150°) = 39.75°, 46.23°, 67.45°, 81.24°, 85.69°, 103.48°, 117.67°, 122.78°, and 66.76° (see embedded in Figure S3). The XRD pattern of our as-received Pt/C catalyst showed crystalline peaks at 2θ of 21.89°, 39.79°, 46.27°, and 67.47° (see Figure 3S), which closely matched the XRD standard pattern of Pt/C at low angles of 20-80°. Similarly, all the activated carbons exhibited similar morphology, with peaks located at 2θ = 31-38°, 47°, 56°, 62°, and 67-69°. The result confirms the existing of Pt supported on carbon without crystalline impurities.

The surface morphology of the catalyst was examined using field emission scanning electron microscopy with energy-dispersive X-ray spectroscopy (FE-SEM-EDS), as presented in Figure S4. At magnifications of 5000x and 10,000x, a porous structure with microparticle deposition was observed (see Figure S4(a-b)). This is a characteristic feature of platinum metal supported on activated carbon. Furthermore, the platinum distribution on the activated carbon support appeared to be uniform, as illustrated by the elemental mapping of carbon and platinum (Figure S4(c-d)). All the characterization results confirmed that the

Pt/C catalyst was suitable for the reaction testing, specifically the deoxygenation of crude palm kernel oil.

3.2 Characterization of the raw material

The composition analysis of CPKO, summarized in Table 2, was conducted using GC-MS following the methodology of Makcharoen et al. (2021) [15]. The results revealed that the majority of carbon atoms in CPKO (approximately 74.74%) were present in the carbon chain length ranging from C_8 to C_{16}. These carbon sources are crucial for the sustainable production of biojet fuel, emphasizing the potential of CPKO as a green feedstock. In contrast, crude palm oil (CPO) exhibited a relatively low content of C_8 to C_{16}, making it less suitable for biojet fuel applications. However, CPO has been recognized as a suitable raw material for the production of green diesel [21].

The acidity of CPKO was 33.95 mg_{KOH}/g_{oil}, indicating a high level of free fatty acids (FFA) compared to other crude palm-based feedstocks. These FFA compounds can undergo conversion into oxygen-free hydrocarbons through three primary reactions: hydrodeoxygenation (HDO), decarbonylation (DCO), and decarboxylation (DCX), under a hydrogen atmosphere (Valencia et al., 2018) [22]. Additionally, catalytic cracking may occur under nitrogen atmosphere at high temperatures (Johansson et al., 2023) [23].

3.3 Effect of reaction temperature

The reaction temperature was identified as a crucial factor in biojet synthesis, as it directly influenced the reaction pathway and product distribution. Therefore, it was prioritized for investigation and optimization. Throughout the experiments, the color of the liquid product and the yield of biojet product were monitored. The experimental setup involved a constant CPKO flow rate of 0.02 mL/min, with a gas flow rate of 17.5 mL/min (either hydrogen or nitrogen). In the literature, it was reported that the high temperature (> 300ºC) was required to achieve the high biojet yield [26, 27]; however, the excess thermal cracking of liquid products (> 400ºC) could occur [28]. In addition, using the temperature exceeding 400ºC could promote the deactivation of catalyst [29]. Hence, in this work, two different temperatures, 380°C and 400°C, were chosen for the reaction, while maintaining a pressure of 250 psi. The synthesis process was conducted both with and without a catalyst, and the specific experimental conditions were indicated by the codes as summarized in Table 1.

Figure 2 illustrates the liquid product collected during the 2-10 h time-on-stream period, with each sample being collected for 1 h, under the catalyst-free system. The time-on-stream started when CPKO was introduced into the reactor. In experiments conducted with hydrogen gas, the liquid product from P4 (400°C) exhibited a slight brownish color, whereas P2 (380°C) produced a yellowish product. When nitrogen gas was used, the product from P1 (380°C) appeared yellowish-brown. Elevating the reaction temperature to 400°C (P3) resulted in a dark brown liquid product, primarily due to thermal cracking at higher temperatures, particularly in the presence of an inert gas environment [30]. Since in the N_2 atmospheric system, primarily pyrolysis reactions (thermal cracking) occurred. The dark brown liquid (pyrolysis oil) was a major product of this process. Moreover, the yellowish liquid product was attributed to the high content of unreacted CPKO under catalyst-free conditions. The liquid yield and the yield of biojet-range product (nC_8-nC_{16}) were measured for P1-P4. The liquid yield remained relatively stable in the range of 72-75% for all conditions (data not shown). This means that the gas and solid products did not significantly increase under these temperatures. However, the change of liquid compositions (mostly biojet-range product) was observed, strongly influenced by the type of gas utilized in the process, as depicted in Figure 3. It was shown that hydrogen gas led to approximately twice the yield compared to nitrogen gas. Notably, varying the reaction temperature (380-400°C) did not produce a significant difference in biojet yield. Therefore, the catalytic system was required along with the H_2 source to approach the high biojet yield via catalytic hyproprocessing reactions (HDO, DCO, and DCX).

Similar experiments were conducted by introducing a catalyst (Pt/C), with a fixed amount of 0.04 g for each experiment. These conditions were denoted as c-P1 to c-P4. Figure 4 demonstrates a marked improvement in liquid yield, particularly when hydrogen gas was employed at 400°C (c-P4). Upon comparing the biojet yields, it was evident that the use of hydrogen gas in hydroprocessing reactions with CPKO significantly enhanced biojet production, reaching approximately 80% yield for c-P4. It is worth mentioning that the reaction kinetics were enhanced with increasing reaction temperature. The liquid samples in all cases exhibited a slightly yellowish hue, as depicted in the embedded pictures of Figure 4, which differed from those obtained without the use of catalyst. In contrast to the non-catalytic process described earlier, a significant difference was observed when the temperature was changed from 400°C to 380°C. The biojet yield decreased from 80% to 55% for hydrogen gas conditions due to the presence of catalyst. However, at 380°C (c-P2), the biojet yield was only slightly higher than that of P2 without the catalyst. This effect was less pronounced in the case of nitrogen gas, indicating a lower activation energy. Notably, the biojet yield remained comparable to that obtained without the catalyst.

3.4 Effect of ratio between hydrogen and nitrogen

The presence of hydrogen gas is critical in hydroprocessing and constitutes a major component in the raw material cost since the major role of H_2 was to promote the HDO reaction (Kubička et al., 2014) [31]. The deactivation of catalyst (coke formation) was also

mitigated. As a result, the choice of gas in CPKO-based biojet production can substantially impact both production performance and cost. In this work, the biojet production under the gas mixture of hydrogen-nitrogen atmosphere was demonstrated experimentally in order to improve the environmental and economic sustainability of the production. To investigate this, a series of experiments were conducted, varying the molar ratio between hydrogen and nitrogen. The operating conditions remained the same as c-P4, except for the gas type utilized. The results are presented in Figure 5.

The findings clearly indicated that using pure hydrogen gas yielded the highest biojet production (approximately 80%). This was in line with the related literature involving the use of Pt-based catalysts for hydroprocessing reaction [32, 33]. In this path way, the H_2 was required to cleave carbon–oxygen and carbon–carbon bonds. However, a respectable yield of 60% was achieved with a 75:25 hydrogen-to-nitrogen ratio. Further decreasing the ratio led to lower yields, with the lowest yield of approximately 29% observed when using nitrogen gas alone. These trends suggested that hydrocracking was the preferred pathway for biojet production over catalytic cracking [34]. Similar results were reported in the study by Mapiour et al. (2009) [35], where the impact of an H_2-CH_4 gas mixture on hydroprocessing reactions (hydrodesulfurization, hydrodenitrogenation, and hydrodearomatization) was examined. The conversion rates significantly decreased when the purity of hydrogen was reduced. However, increasing the total pressure helped mitigate this negative effect. Therefore, a hydrogen-to-nitrogen ratio of 75:25 was chosen for economic reasons while maintaining satisfactory biojet yields. Further experiments were conducted with the aim of improving reaction performance.

3.5 Effect of pressure

Based on the simulation results obtained from Aspen Plus (version 12) with the nonrandom two-liquid (NRTL) thermodynamic model, it was found that CPKO remained in the liquid phase throughout our study. The hydrogenation of unsaturated oil to FFA was the initial reaction, followed by liquid-phase deoxygenation reactions (DCX and DCO) of fatty acids to straight-chain alkanes [36, 37]. The amount of hydrogen adsorbed on the catalyst surfaces played a crucial role in overall reaction performance. Note that, high surface area and large pore size of this catalyst facilitated the mass transport of reactant molecules on to the catalyst surface (see Table S1). This factor was directly influenced by pressure, specifically the hydrogen partial pressure. Therefore, the effect of pressure was examined in this series of experiments at 250 and 500 psi. It should be noted that the boiling points of FFA present in CPKO at 250 and 500 psi were approximately 480°C and 530°C, respectively. Generally, the liquid-phase DCX of vegetable oil at 300 to 360°C required a total pressure ranging from 246 to 500 psi [38].

In this particular set of experiments, the reaction temperature, catalyst amount, H_2-to-N_2 ratio, gas flow rate, and CPKO flow rate were set at 400°C, 0.04 g, 75:25, 17.5 mL/min, and 0.02 mL/min, respectively. The results are compared in Figure 6. The biojet yield was

approximately 60% for both 250 and 500 psi. Although there was no significant change in biojet yield due to the pressure difference, the color of the product clearly differed. The product obtained at 500 psi was clear and colorless, while the product at 250 psi appeared yellowish and transparent. The chromatograms of these products are presented in Figure 7. At 500 psi, the product distribution was shifted towards the left side of the chromatogram, and the content of unreacted CPKO was reduced, indicating a higher degree of cracking. It is worth noting that iso-C_{11} was the predominant component in both samples. This was likely the result of DCX of dodecanoic acid (no water was detected), followed by isomerization. However, the peaks representing n-C_{14} and iso-C_{14} were relatively small, suggesting that tetradecanoic acid was cracked into smaller molecules. The peaks of C_{17} and C_{18} at 500 psi were smaller compared to those at 250 psi, indicating that heavy product molecules at 250 psi contained oleic acid in the glycerol backbone. The content of iso-C_{15} was significantly increased at 500 psi, which was attributed to the DCX and isomerization of hexadecanoic acid. Overall, while higher operating pressure would raise energy requirements and equipment costs for safety of the operation, a total pressure of 500 psi was selected for subsequent experiments in this study due to the observed differences in product quality.

3.6 Effect of gas flow rate

The subsequent variable under investigation was the gas flow rate. The experimental conditions remained consistent with those described in Section 3.5, except for the constant flow rates of the gas mixture (H_2-to-N_2 ratio of 75:25) set at 17.5 mL/min and 25 mL/min for each experiment. This variation affected the rate at which hydrogen was supplied to the reactions and the residence time of the mixture in the reactor. Figure 8 illustrates the results, indicating that changing the gas flow rate did not result in a significant difference in biojet yield. However, the yield remained stable throughout the experiments. The visual appearance of the liquid product was similar, as depicted in the embedded pictures in Figure 8. Notably, at a flow rate of 25 mL/min, the product appeared slightly more transparent.

Analyzing the chromatogram of the liquid product obtained at 25 mL/min, it was observed that the peaks corresponding to n-C_{18} and iso-C_{18} were considerably smaller compared to the product obtained using a gas flow rate of 17.5 mL/min. Conversely, the peaks representing C_{17} were relatively reduced for the case of 25 mL/min, indicating a greater degree of DCX of oleic acid followed by isomerization. The same trend was observed for the peaks of C_{16} and C_{15}. These results suggested that the increased rate of hydrogen supply facilitated more effective progress of the reactions despite the shortened residence time in the reactor. Owing to the significant rise in the proportion of C12, C13, and C15 relative to C16, a flow rate of 25 mL/min was chosen for further enhancement.

3.7 Effect of CPKO flow rate

The productivity of biojet production from CPKO is influenced by the feed flow rate. To investigate this, we compared the performance of two different flow rates: 0.02 mL/min and 0.03 mL/min. All other reaction parameters, including temperature, pressure, H_2-to-N_2 ratio, gas flow rate, and catalyst amount, were held constant at 400 ºC, 500 psi, 75:25, 25 mL/min, and 0.04 g, respectively.

The findings, illustrated in Figure 9, demonstrate that at a CPKO flow rate of 0.02 mL/min, the resulting liquid product was colorless and transparent, exhibiting a biojet yield of approximately 59%. Conversely, elevating the CPKO flow rate to 0.03 mL/min increased the production rate of liquid product but significantly decreased the biojet yield to 26%. Moreover, the product had a yellowish tint. The chromatogram displayed in Figure 10 revealed a notable presence of CPKO in the sample at the higher flow rate. Peaks representing C11 to C17 were significantly reduced, while heavier molecules were detected, suggesting inadequate residence time for effective hydrotreating reactions.

Thus, based on this work, the optimal conditions for biojet production from CPKO using Pt/C catalyst were determined as 400ºC, 500 psi, an H_2-to-N_2 ratio of 75:25, a gas flow rate of 17.5 mL/min, and a CPKO flow rate of 0.02 mL/min. The liquid product obtained under these conditions was further analyzed for oxygen content and acid value. It was found that the oxygen content in the oil was reduced by 50.20% compared to CPKO, indicating successful deoxygenation in the system. However, the acid value of the product was 100.53 mg_{KOH}/g_{oil}, whereas CPKO had an acid value of 33.95 mg_{KOH}/g_{oil}. This suggests that a significant fraction of the product resulting from the beta elimination of triglycerides did not undergo further chemical transformations. Due to its high acid value, this product cannot be used directly. Additional reactions, such as cracking, dehydration, isomerization, and aromatization, may be employed to enhance the product's properties, similar to a second hydrogenation process.

3.8 Performance of various systems for biojet production

Studies have been conducted on biojet production from palm oil and CPKO in continuous flow reactors using Pt as a catalyst. In this section, we compared the performance of our system with recent literature in various aspects such as operating conditions, biojet yield and productivity, as summarized in Table 3. Previous studies have employed Pt/γ-Al_2O_3 and PtRe/USY catalysts at relatively low temperatures (295-380ºC) using palm oil as the feedstock. However, these systems required a large amount of catalyst (1.2-2.4 g), resulting in relatively low productivity (< 40 $g_{product}/g_{cat}$-h).

Makcharoen et al. (2021) [15] utilized Pt/C catalyst at a relatively high temperature (420ºC)) to convert CPKO into biojet, achieving a yield of 58% and a productivity of 186.4

$g_{product}/g_{cat}$-h. In our work, a smaller amount of catalyst (0.04 g) was used at a lower temperature (400^{o}C), leading to a higher weight hourly space velocity (WHSV). Particularly interesting is the high yield (80%) and productivity (447.6 $g_{product}/g_{cat}$-h) observed when hydrogen gas was used. The use of an H_2-N_2 gas mixture also yielded favorable results in terms of yield (59%) and productivity (330.6 $g_{product}/g_{cat}$-h). The improvement of our proposed process might be implemented by improving the catalytic activity such as using bimetallic catalysts [8, 39] or bifunctional catalysts [40]. These findings indicate the potential of our system for developing a pilot-scale biojet production system.

4. Conclusions

This study has introduced a novel approach to enhance the sustainability and cost-effectiveness of biojet production. The research focused on continuous biojet production using Crude Palm Kernel Oil (CPKO) as a feedstock, conducted using a fixed-bed reactor packed with a commercial Pt/C catalyst, operating under an N_2-H_2 environment. Various operating parameters, including reaction temperature, pressure, gas molar ratio, and reactant flow rates, were systematically investigated and optimized based on the biojet yield. The findings underscored the potential of CPKO as a promising carbon source for biojet production. Moreover, the use of nitrogen was demonstrated as an effective hydrogen substitute, with a 75:25 ratio (hydrogen-to-nitrogen) providing satisfactory biojet yields. The optimal conditions for achieving a remarkable 59% biojet yield were determined, which included a reaction temperature of 400°C, a pressure of 500 psi, a CPKO flow rate of 0.02 mL/min, and a gas flow rate of 25 mL/min. Notably, a deoxygenation degree of 50.2% and a productivity of 330.6 gproduct/gcat-h were evaluated. This proposed process is promising for biojet production from various vegetable oils. However, it is important to acknowledge that further advancements are necessary to increase biojet yields. Exploring innovative catalysts, such as bimetallic catalysts, or integrating hydrogen donor solvents, presents intriguing avenues to address this challenge and advance the field of sustainable biojet production.

Acknowledgements

The authors acknowledge the financial support from the National Research Council of Thailand (NRCT) and Kasetsart University Research and Development Institute (KURDI) through the Reinventing University Program.

Declaration of generative AI and AI-assisted technologies in the writing process

During the preparation of this work the authors used ChatGPT in order to rewrite sentences in order to be grammatically correct. After using this tool/service, the authors reviewed and edited the content as needed and take full responsibility for the content of the publication.

References

[1] Kober T, Schiffer HW, Densing M, Panos E, Global energy perspectives to 2060 – WEC's World Energy Scenarios 2019. Energy Strategy Rev 2020;31:100523. https://doi.org/10.1016/j.esr.2020.100523

[2] Gutiérrez-Antonio C, Gómez-Castro FI, Lira-Flores JA, Hernández S. A review on the production processes of renewable jet fuel. Renew and Sustain. Energy Rev 2017;79:709-729. https://doi.org/10.1016/j.rser.2017.05.108

[3] Itthibenchapong V, Srifa A, Kaewmeesri R, Kidkhunthod P, Faungnawakij K. Deoxygenation of palm kernel oil to jet fuel-like hdrocarbons using Ni-MoS_2/γ-Al_2O_3 catalysts. Energy Convers Manag 2017;134:188-196. https://doi.org/10.1016/j.enconman.2016.12.034

[4] Donoso D, Bolonio D, Ballesteros R, Lapuerta M, Canoira L. Hydrogenated orange oil: A waste derived drop-in biojet fuel. Renew Energy 2022;188:1049-1058. https://doi.org/10.1016/j.renene.2022.02.078

[5] Sousa FP, Silva LN, Reznde DB, Oliveira LCA, Pasa VMD. Simultaneous deoxygenation, cracking and isomerization of palm kernel oil and palm olein over beta zeolite to produce biogasoline, green diesel and biojet-fuel. Fuel 2018;223:149-156. https://doi.org/10.1016/j.fuel.2018.03.020

[6] Vela-García N, Bolonio D, García-Martínez MJ, Ortega MF, Streitwieser DA, Canoira L. Biojet fuel production from oleaginous crop residues: thermoeconomic, life cycle and flight performance analysis. Energy Convers Manag 2021;244:114534. https://doi.org/10.1016/j.enconman.2021.114534

[7] Rambabu K, Bharath G, Sivarajasekar N, Velu S, Sudha PN, Wongsakulphasatch S, Banat F. Sustainable production of bio-jet fuel and green gasoline from date palm seed oil via hydroprocessing over tantalum phosphate. Fuel 2023;331:125688. https://doi.org/10.1016/j.fuel.2022.125688

[8] Bharath G, Rambabu K, Hai A, Banat F,Taher H, Schmidt JE, Show PL. Catalytic hydrodeoxygenation of biomass-derived pyrolysis oil over alloyed bimetallic Ni_3Fe

nanocatalyst for high-grade biofuel production. Energy Convers Manag 2020;213:112859. https://doi.org/10.1016/j.enconman.2020.112859

[9] Goh BHH, Chong CT, Ong HC, Seljak T, Katrašnik T, Józsa V, Ng JH, Tian B, Karmarkar S, Ashokkumar V. Recent advancements in catalytic conversion pathways for synthetic jet fuel produced from bioresources. Energy Convers Manag 2022;251:114974. https://doi.org/10.1016/j.enconman.2021.114974

[10] Why ESK, Ong HC, Lee HV, Chen WH, Asikin-Mijan N, Varman M. Conversion of bio-jet fuel from palm kernel oil and its blending effect with jet A-1 fuel. Energy Convers Manag

2021;243, 114311. https://doi.org/10.1016/j.enconman.2021.114311

[11] Zhang J, Zhao C. A new approach for bio-jet fuel generation from palm oil and limonene in absence of hydrogen. Chem Commun 2015;51:17249-17252. https://doi.org/10.1039/C5CC06601H

[12] Martinez-Hernandez E, Ramírez-Verduzco LF, Amezcua-Allieri MA, Aburto J. Process simulation and techno-economic analysis of bio-jet fuel and green diesel production-minimum selling prices. Chem Eng Res Des 2019;146:60-70.

[13] Wei H, Liu W, Chen X, Yang Q, Li J, Chen H. Renewable bio-jet fuel production for aviation: A review. Fuel 2019;254:115599. https://doi.org/10.1016/j.fuel.2019.06.007

[14] https://www.zauba.com

[15] Makcharoen M, Kaewchada A, Akkarawatkhoosith N, Jaree A. Biojet fuel production via deoxygenation of crude palm kernel oil using Pt/C as catalyst in a continuous fixed bed reactor. Energy Convers Manag X 2021;12:100125. https://doi.org/10.1016/j.ecmx.2021.100125

[16] Bharath G, Rambabu K, Hai A, Ponpandian N, Schmidt JE, Dionysiou DD, et al.

Dual-functional paired photoelectrocatalytic system for the photocathodic reduction of CO2 to fuels and the anodic oxidation of furfural to value-added chemicals. Appl Catal B Environ 2021;298:120520. https://doi.org/10.1016/j.apcatb.2021.120520

[17] Bharath G; Rambabu K. Hai A, Banat F; Rajendran S; Dionysiou DD, et al. High-performance and stable Ru-Pd nanosphere catalyst supported on two-dimensional boron nitride nanosheets for the hydrogenation of furfural via water-mediated protonation. Fuel 2021;290: 119826. https://doi.org/10.1016/j.fuel.2020.119826

[18] Jeon KW, Park HR, Lee YL, Kim JE, Jang WJ, Shim JO, Roh HS. Deoxygenation of non-edible fatty acid for green diesel production: Effect of metal loading amount over

Ni/MgO–Al_2O_3 on the catalytic performance and reaction pathway. Fuel 2022;311:122488. https://doi.org/10.1016/j.fuel.2021.122488

[19] Bangjang T, Kaewchada A, Jaree A. Hydroprocessing of palm oil using Rh/HZSM-5 for the production of biojet fuel in a fixed bed reactor. Can J Chem Eng 2020;99:435-46. https://doi.org/10.1002/cjce.23877

[20] Kim MY, Choi JS, Toops TJ, Jeong ES, Han SW, Schwartz V, Chen J. Coating SiO_2 support with TiO_2 or ZrO_2 and effect on structure and CO oxidation performance of Pt catalysts. Catal 2013;3:88-103. https://doi.org/10.3390/catal3010088

[21] Mahdi HI, Bazargan A, McKay G, Azelee NIW, Meili L. Catalytic deoxygenation of palm oil and its residue in green diesel production: A current technological review. Chem Eng Res Des 2021;174:158-187. https://doi.org/10.1016/j.cherd.2021.07.009

[22] Valencia D, García-Cruz I, Uc VH, Ramírez-Verduzco LF, Amezcua-Allieri MA, Jorge Aburto J. Unravelling the chemical reactions of fatty acids and triacylglycerides under hydrodeoxygenation conditions based on a comprehensive thermodynamic analysis. Biomass Bioenergy 2018;112:37-44. https://doi.org/10.1016/j.biombioe.2018.02.014

[23] Johansson AC, Bergvall N, Molinder R, Wikberg E, Niinipuu M, Sandström L. Comparison of co-refining of fast pyrolysis oil from Salix via catalytic cracking and hydroprocessing. Biomass Bioenergy 2023;172:106753. https://doi.org/10.1016/j.biombioe.2023.106753

[24] Ejeromedoghene O. Acid-catalyzed transesterification of Palm Kernel Oil (PKO) to biodiesel. Mater Today: Proceedings 2021;47:1580-1583. https://doi.org/10.1016/j.matpr.2021.04.042

[25] Elsheikh YA, Man Z, Bustam A, Yusup S, Akhtar FH, Mohamed IK. Evaluation of catalytic activity of two functionalized imidazolium ionic liquids for biodiesel fuel production by a two-stage process. J Chem Tech Biotech 2013;89:998-1006. https://doi.org/10.1002/jctb.4191

[26] Vonortas A, Papayannakos N. Hydrodesulphurization and hydrodeoxygenation of gasoil-vegetable oil mixtures over a Pt/γ-Al_2O_3 catalyst. Fuel Process Technol 2016;150:126-131. https://doi.org/10.1016/j.fuproc.2016.05.013

[27] Li X, Chen Y, Hao Y, Zhang X, Du J, Zhang A. Optimization of aviation kerosene from one-step hydrotreatment of catalytic Jatropha oil over SDBS-Pt/SAPO-11 by response surface methodology. Renew Energy, 2019;139:551-559. https://doi.org/10.1016/j.renene.2019.01.085

[28] Žula M, Grilc M, Likozar B. Hydrocracking, hydrogenation and hydro-deoxygenation of fatty acids, esters and glycerides: Mechanisms, kinetics and transport phenomena

Chem Eng J 2022;444:136564. https://doi.org/10.1016/j.cej.2022.136564

[29] Rahmawati Z, Santoso L, McCue A, Jamari NLA, Ninglasari SY, Gunawan T, Fansuri H. Selectivity of reaction pathways for green diesel production towards biojet fuel applications. RSC Adv 2023;13:13698-13714. https://doi.org/10.1039/D3RA02281A

[30] Fimberger J, Swoboda M, Reichhold A. Thermal cracking of canola oil in a continuously operating pilot plant. Powder Tech 2017;316:535-541. https://doi.org/10.1016/j.powtec.2016.10.030

[31] Kubička D, Horáček J, Setnička M, Bulánek R, Zukal A, Kubičková I. Effect of support-active phase interactions on the catalyst activity and selectivity in deoxygenation of triglycerides. Appl Cat B: Environ 2014;145:101-107. https://doi.org/10.1016/j.apcatb.2013.01.012

[32] Wang WC, Thapaliya N, Campos A, Stikeleather LF, Roberts WL. Hydrocarbon fuels from vegetable oils via hydrolysis and thermo-catalytic decarboxylation. Fuel 2012.;95:622-629. https://doi.org/10.1016/j.fuel.2011.12.041

[33] Le VN, Phan DP, Kim SS, Lee EY, Kim J. Optimization of operating conditions for anisole hydrodeoxygenation reaction over Zr-based metal–organic framework supported Pt catalyst. Fuel Process Technol 2022;238:107477. https://doi.org/10.1016/j.fuproc.2022.107477

[34] Nkazi D, Mukaya HE, Molefe M. Method selection for bio-jet and bio-gasoline fuels production from castor oil: A Review. Energy Fuels 2019;33:5918-5932. https://doi.org/10.1021/acs.energyfuels.9b00384

[35] Mapiour M, Sundaramurthy V, Dalai AK, Adjaye J. Effect of Hydrogen Purity on Hydroprocessing of Heavy Gas Oil Derived from Oil-Sands Bitumen. Energy Fuels 2009;23: 2129-2135. https://doi.org/10.1021/ef801005m

[36] Snåre M, Kubičková I, Mäki-Arvela P, Chichova D, Eränen K, Murzin DY, Catalytic deoxygenation of unsaturated renewable feedstocks for production of diesel fuel hydrocarbons. Fuel 2008;87:933-945. https://doi.org/10.1016/j.fuel.2007.06.006

[37] Wang Y, He T, Liu K, Wu J, Fang Y. From biomass to advanced bio-fuel by catalytic pyrolysis/hydro-processing: Hydrodeoxygenation of bio-oil derived from biomass catalytic pyrolysis. Bioresour Technol 2012;108: 280-284. https://doi.org/10.1016/j.biortech.2011.12.132

[38] Kubičková I, Snåre M, Eränen K, Mäki-Arvela P, Murzin DY, Hydrocarbons for diesel fuel via decarboxylation of vegetable oils. Catal. Today 2005;106:197-200. https://doi.org/10.1016/j.cattod.2005.07.188

[39] Bharath G, Rambabu K, Hai A, Morajkar PP, Salkar VA, Hasan SW, Show PL, Banat F. Highly selective etherification of fructose and 5-hydroxymethylfurfural over a novel Pd-Ru/MXene catalyst for sustainable liquid fuel production. Int J Energy Res 2021;45:14680-14691. https://doi.org/10.1002/er.6743

[40] Bharath G, Hai A, Rambabu K, Kallem P, Haija MA, Banat F, Theerthagiri J, Choi MY. Fabrication of $Pd/MnFe_2O_4$ bifunctional 2-D nanosheets to enhance the yield of HCOOH from CO_2 cathodic reduction paired with anodic oxidation to CH_3OH. Fuel 2022;311;122619. https://doi.org/10.1016/j.fuel.2021.122619

[41] Lee K, Lee ME , Kim JK, Shin B, Choi M. Single-step hydroconversion of triglycerides into biojet fuel using CO-tolerant PtRe catalyst supported on USY. J Catal 2019;379:180-190. https://doi.org/10.1016/j.jcat.2019.09.043

[42] Kim TH, Lee K, Kim MY, Chang YK, Choi M. Effects of Fatty Acid Compositions on heavy oligomer formation and catalyst deactivation during deoxygenation of triglycerides. ACS sustain chem eng 2018;6:17168-17177. https://doi.org/10.1021/acssuschemeng.8b04552

Figure captions

Figure 1 Experimental apparatus.

Figure 2 Liquid products collected hourly from 2-10 h for different experimental conditions (P1-P4).

Figure 3 Biojet-range yield (nC_8-nC_{16}) using different reaction temperatures under catalyst-free system (P1-P4).

Figure 4 (a) Biojet yield (nC_8-nC_{16}) using different reaction temperatures under catalyst system (c-P1 to c-P4).

Figure 5 Biojet yield (nC_8-nC_{16}) using different gas compositions (c-P3-c-P7).

Figure 6 Liquid and Biojet yield (nC_8-nC_{16}) obtained at 250 and 500 psi (c-P5, c-P8).

Figure 7 Chromatograms of liquid product obtained at 250 psi and 500 psi (c-P5, c-P8).

Figure 8 Biojet yield (nC8-nC16) obtained at different gas flow rates (c-P8, c-P9).

Figure 9 Biojet yield (nC_8-nC_{16}) obtained at different CPKO flow rates (c-P9, c-P10).

Figure 10 Chromatogram of liquid product obtained at the CPKO flow rate of 0.02 and 0.03 mL/min (c-P9, c-P10).

List of tables

Highlight

1. Biojet production from crude palm kernel oil under H_2-N_2 atmosphere was demonstrated.
2. Effects of operating parameters on the yield of biojet were investigated and optimized.
3. The high productivity of 330.6 $g_{product}/g_{cat}$-h was achieved.

Table 1 Reaction conditions for deoxygenation of CPKO to biojet fuel.

Code	Temp (℃)	Pressure psi	Pt/C (g)	H_2:N_2 molar ratio	Gas flow rate (mL/min)	Liquid flow rate (mL/min)
P1	380	250	-	0:100	17.5	0.02
P2	380	250	-	100:0	17.5	0.02
P3	400	250	-	0:100	17.5	0.02
P4	400	250	-	100:0	17.5	0.02

c-P1	380	250	0.04	0:100	17.5	0.02
c-P2	380	250	0.04	100:0	17.5	0.02
c-P3	400	250	0.04	0:100	17.5	0.02
c-P4	400	250	0.04	100:0	17.5	0.02
c-P5	400	250	0.04	75:25	17.5	0.02
c-P6	400	250	0.04	50:50	17.5	0.02
c-P7	400	250	0.04	25:75	17.5	0.02
c-P8	400	500	0.04	75:25	17.5	0.02
c-P9	400	500	0.04	75:25	25	0.02
c-P10	400	500	0.04	75:25	25	0.03

663

664

665 **Table 2** Fatty acid composition of various CPKO and CPO feedstocks.

Properties/composition	CPKO[a]	CPKO [24]	CPO [25]
Average molecular weight (g/mol)	736.4	704	NA
Acid value (mg_{KOH}/g_{oil})	33.95	8.4	6.98

Fatty acid composition (wt.%)			
Octanoic acid (C8:0)	0.95	2.9	-
Decanoic acid (C10:0)	3.23	5.2	-
Dodecanoic acid (C12:0)	32.78	46.5	0.4
Tetradecanoic acid (C14:0)	20.25	19	1.26
Hexadecanoic acid (C16:0)	14.12	7.3	46.90
Stearic acid (C18:0)	4.06	2.1	4.59
Oleic acid (C18:1)	20.72	14.0	36.85
Linoleic acid (C18:2)	1.34	1.8	9.09
cis-11-eicosenoic acid (C20:1)	0.17	-	0.39
Heneicosanoic acid (C21:0)	0.60	-	-
Others	1.78	1.2	0.52

666 [a] This work

667

668 **Table 3** Performance of biojet production systems

Reactant	Catalyst	Conditions	Reactor	Biojet Yield (%wt)	Productivity $g_{product}/g_{cat}$-h	Ref.

Palm oil	PtRe/USY (1.2 g)	295 ◦C, 725 psi, H_2 flow 232 mL/min, WHSV = 2 h^{-1}	Fixed-bed	41%	20	[41]
Palm oil	Pt/γ-Al_2O_3 (2.4 g)	380 ◦C, H_2 flow 46 mL/min, 290 psi, WHSV = 1 h^{-1}	Fixed-bed	36%	36	[42]
CPKO	Pt/C (0.07 g)	420ºC 500 psi , H_2 17.50 mL/min WHSV = 16 h^{-1}	Fixed-bed	58%	186.4	[15]
CPKO	Pt/C (0.04 g)	400ºC 500 psi, H_2 17.50 mL/min WHSV = 22.18 h^{-1}	Fixed-bed	80%	447.6	This work
CPKO	Pt/C (0.04 g)	400ºC 500 psi, H_2:N_2 = 3:1, 25 mL/min WHSV = 22.18 h^{-1}	Fixed-bed	59%	330.6	This work

669

670

671

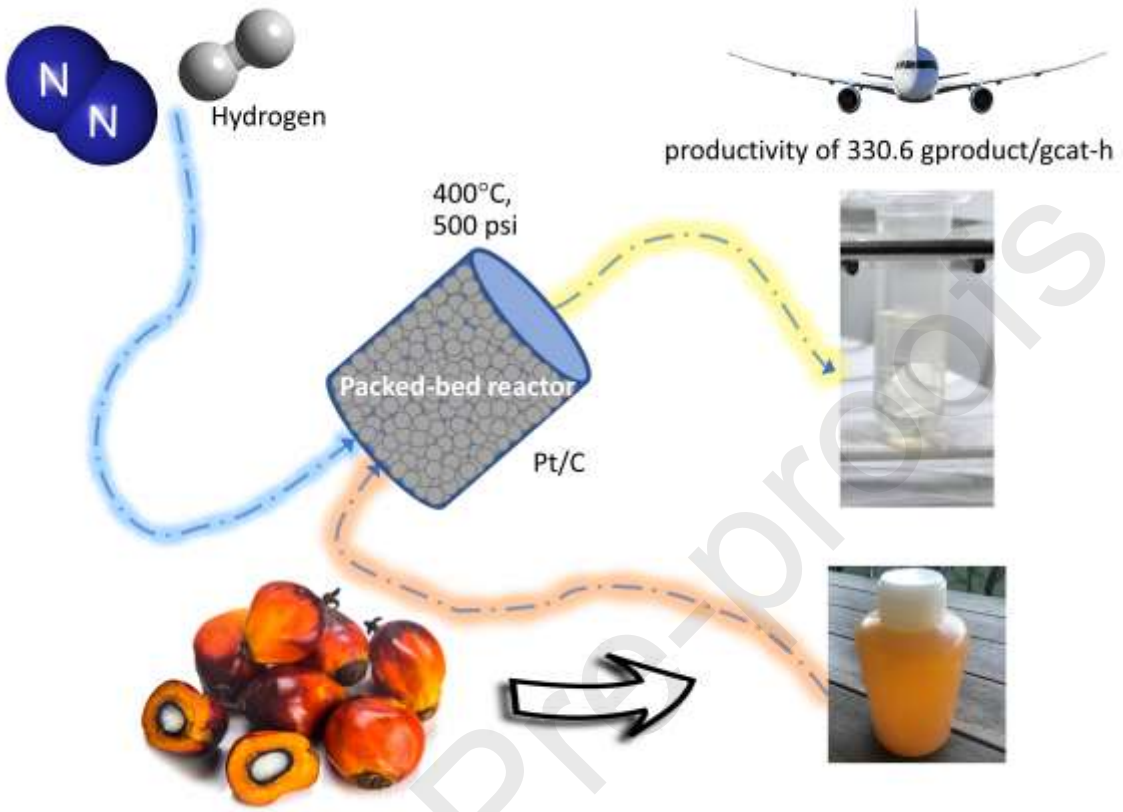

672